



# Magneto Prandtl nanofluid past a stretching surface with non-linear radiation and chemical reaction

K.Ganesh Kumar <sup>a</sup>, G.K.Ramesh <sup>b,\*</sup>, S.A. Shehzad <sup>c</sup> and B.J.Gireesha <sup>d</sup>

<sup>a</sup>Department of Mathematics, S.J.M. Institute of Technology, Chitradurga-577501, Karnataka, INDIA

<sup>b</sup>Department of Mathematics, K.L.E Society's J.T. College, Gadag-582102, Karnataka, INDIA

<sup>c</sup>Department of Mathematics, COMSATS Institute of Information Technology, Sahiwal 57000, Pakistan

<sup>d</sup>Department of Studies and Research in Mathematics, Kuvempu University, Shankaraghatta-577 451, Shimoga, Karnataka, INDIA.

---

**Article info:**

Received: 00/00/2000

Accepted: 00/00/2018

Online: 00/00/2018

**Keywords:**

MHD flow,  
Prandtl nanofluid,  
Nonlinear thermal  
radiation,  
chemical reaction,  
slip effect.

**Abstract**

In this article, we examined the behavior of chemical reaction effect on a magnetohydrodynamic Prandtl nanofluid flow due to stretchable sheet. Non-linear thermally radiative term is accounted in energy equation. Constructive transformation is adopted to formulate the ordinary coupled differential equations system. This system of equations is treated numerically through Runge Kutta Fehlberg-45 method based shooting method. The role of physical constraints on liquid velocity, temperature and concentration are discussed through numerical data and plots. Also the skin friction co-efficient, local Nusselt number and local Sherwood numbers is calculated to study the flow behavior at the wall, which is also presented in tabular form. A comparative analysis is presented with the previous published data in special case for the justification of present results. Output reveals that for larger values of elastic and Prandtl parameter enhanced the thickness of momentum layer and reduces the rates of both heat and mass transport. Also increment of slip parameter decelerated both temperature and concentration filed while nonlinear form thermal radiation rapidly increases the temperature.

---

**Nomenclature**

$A$  and  $c$  Material constants

$b$  Constant

$B_0$  Magnetic field

$B$  Thermal slip parameter

$C$  Nanoparticle volume fraction

$C_w$  Concentration at wall

$C_\infty$  Ambient nanofluid volume fraction

$C_{fx}$  Skin friction coefficient

$c_p$  Specific heat coefficient

$D$  Solutal slip parameter

$D_B$  Coefficient of Brownian diffusion

$D_T$  Coefficient of thermophoretic diffusion

$K$  Chemical reaction coefficient

$K_1$  and  $K_2$  Slip factor

$k$  Thermal conductivity

$k^*$  Mean absorption coefficient

$Le$  Lewis number

---

\*Corresponding author

Email address: gkrmaths@gmail.com

$Nb$	Brownian motion parameter
$Nt$	Thermophoresis parameter
$Nu_x$	Local Nusselt number
$Pr$	Prandtl number
$q_r$	Radiative heat flux
$q_w$	Heat flux
$q_m$	Mass flux
$Ra$	Radiation parameter
$Re_x$	Local Reynolds number
$Sh_x$	Local Sherwood number
$T$	Fluid temperature
$T_w$	Surface temperature
$T_\infty$	Ambient surface temperature
$u, v$	Velocity components
$U_w$	Stretching sheet
$x, y$	Coordinates

**Greek symbols**

$\theta$	Dimensionless temperature
$\theta_w$	Temperature ratio parameter
$\phi$	Dimensionless nanoparticle volume fraction
$\nu$	Kinematic viscosity of the fluid
$\beta$	Volumetric coefficient
$\mu$	Dynamic viscosity
$\sigma^*$	Stefan–Boltzmann constant
$\tau$	Ratio of effective heat capacity of nanoparticle to ordinary liquid
$\tau_w$	Shear stress along the wall
$\alpha$	Prandtl parameter
$\beta$	Elastic parameter
$\alpha_1$	Liquid thermal diffusivity
$\lambda$	Mixed convection parameter
$\gamma$	Chemical reaction parameter
$\rho$	Density of the fluid

**1. Introduction**

Significant attention has been given in the recent years to address the behavior of flow and heat analysis on nanofluids. The reason is ordinary fluids having the low thermal conductivity. By adding the nano size particles in an ordinary fluid, thermal conductivity of liquid enhanced dramatically which was examined by Chio [1]. Comprehensive detail of convective transport in nanofluid has been investigated by Buongiorno [2]. Khan and Pop [3] analyzed the thermoporesis and Brownian

mothion effects on boundary layer flow due to stretching surface. Makinde et al [4] examined the heat transport behavior in nanofluid flow past a convective type heating surface. Sheikholeslami et al [5] provided numerical solution for Magneto nanofluid flow and heat transfer characteristic in a rotating framework. Ramesh et al [6-8] studied the two and three dimensional flow of non-newtonian nanofluid over a different geometry.

Now a day, many researchers are concentrating on exploration of non-Newtonian liquids, because non-Newtonian fluids have multidisciplinary applications in modern industrial and technological products. Few examples of non-Newtonian materials include food, ketchup, shampoos, slurries, granular suspension, paper pulp, paints, polymer solutions, certain oils, and clay coatings. All the features of non-Newtonian liquids cannot be distinguished by a single mathematical relationship. Govardhan et al. [9] initiated the magnetohydrodynamics effects in mixed convective micropolar liquid over moving sheet. Cortell [10] discussed the hydromagnetic power-law liquid flow. Malik et al. [11] employed Keller box technique to study tangent hyperbolic liquid flow under magnetic force induced by moving cylinder. Rehena et al. [12] investigated the Prandtl number effect on assisted convective heat transfer through a solar collector. Akbar at al. [13] studied the magnetohydrodynamic tangent hyperbolic liquid flow towards a stretched sheet with magnetic field. Nasrin and Alim [14] analyzed the Prandtl number effect on free convective flow in a solar collector utilizing nanofluid. Nadeem et al. [15] addressed the importance of stenosis and nanoparticle in peristaltic Prandtl fluid flow.

Thermal radiation has potential role in manufacturing design of nuclear power plants and various engineering processes. Numerous researchers have paid their attention to address the mechanism of thermal radiation. Shehzad et al. [16] reported nonlinear radiation in three dimensional Jeffrey nanofluid flow induced by the bi-directionally moving surface. Influence of nonlinear thermal radiation on Carreau nanofluid over a nonlinear form of stretched

sheet is reported by Zaib et al.[17]. The recent advancements in phenomenon of nonlinear radiation heat transport have been demonstrated in the studies [18-22].The role of slip and thermal jump conditions on heat transport for both Newtonian and non-Newtonian liquid sunder various flow geometries have been reported by various researchers. Wang [23] discussed the partial slip boundary conditions over moving stretched sheet. The effect of slip exponentially boundary layer stretched flow with thermal radiation has described by Swati and Gorla [24]. Fang et al [25] performed the flow past a shrinking sheet by considering second order slip. Bhattacharyya et al [26] explored the slip effects on free stream velocity across a shrinking sheet. Das et al [27] addressed the heat source/sink effect on nanofluid flow in a vertical direction. Kezzar et al. [28] obtained the series solution for flow over a stretchable/shrinkable wall in the presence of nanoparticles. Further Kezzar et al. [29] discussed the heat transport performance on magneto nanofluid flow in a non-parallel plate.

Motivation from the above studies, we want to analyze the importance of chemical reaction and multiple slip effects on Prandtl nanofluid flow past a stretchable surface. In addition, the effect of transverse magnetic field and nonlinear thermal radiation are included. Using suitable similarity variables, the governed partial differential systems are converted into system of non-linear ordinary differential equations and then tackled numerically. The numerical values of the skin friction coefficient and local Nusselt number are also recorded in a tabular form.

## 2. Mathematical analysis

We considered the steady-state incompressible Prandtl nanofluid flow over a stretchable sheet. The  $x$ -axis is along the sheet and  $y$ -axis normal to it. Here the flow generation is because of linear stretching of surface with distance  $x$ , i.e.  $U_w = bx$ . A constant magnetic field with strength  $B_0$  is implemented in transverse flow direction.  $T_w$  is the surface temperature at wall and  $C_w$  the solutal

concentration. At larger distance from surface, temperature and nanoparticle concentration is represented by  $T_\infty$  and  $C_\infty$  respectively.

The continuity, momentum, energy and concentration expressions are described as (see Akbar et al [13])

$$\frac{\partial u}{\partial x} + \frac{\partial v}{\partial y} = 0, \tag{1}$$

$$u \frac{\partial u}{\partial x} + v \frac{\partial u}{\partial y} = \nu \frac{A}{c} \frac{\partial^2 u}{\partial y^2} + \frac{\nu A}{2c^3} \left( \frac{\partial u}{\partial y} \right)^2 \frac{\partial^2 u}{\partial y^2} - \frac{\sigma B_0^2}{\rho} u, \tag{2}$$

$$u \frac{\partial T}{\partial x} + v \frac{\partial T}{\partial y} = \alpha_1 \frac{\partial^2 T}{\partial y^2} + \tau \left[ D_B \frac{\partial C}{\partial y} \frac{\partial T}{\partial y} + \frac{D_T}{T_\infty} \left( \frac{\partial T}{\partial y} \right)^2 \right] - \frac{\partial q_r}{\partial y}, \tag{3}$$

$$u \frac{\partial C}{\partial x} + v \frac{\partial C}{\partial y} = D_B \frac{\partial^2 C}{\partial y^2} + \frac{D_T}{T_\infty} \frac{\partial^2 T}{\partial y^2} + K(C - C_\infty), \tag{4}$$

with the relevant boundary conditions

$$\begin{aligned} u &= u_w, \quad v = 0, \quad T = T_w + K_1 \frac{\partial T}{\partial y}, \\ C &= C_w + K_2 \frac{\partial C}{\partial y} \text{ at } y = 0, \\ u &\rightarrow 0, \quad T \rightarrow T_\infty, \quad C \rightarrow C_\infty \text{ as } y \rightarrow \infty, \end{aligned} \tag{5}$$

here the velocity components are presented by  $u$  and  $v$ ,  $\alpha_1$  for thermal diffusivity,  $\nu = \frac{\mu}{\rho}$  for kinematic viscosity,  $\beta$  for coefficient volumetric thermal expansion,  $\rho$  for liquid density,  $\sigma$  for electrical conductivity,  $A$  and  $c$  for material constants of Prandtl fluid model,  $\tau$  for nanoparticle effective heat capacity of the liquid,  $K$  for chemical reaction coefficient,  $K_1$  and  $K_2$  are thermal and concentration slip factor,  $D_B$  for Brownian diffusion coefficient and  $D_T$  for thermophoresis diffusion coefficient,  $T$  for fluid temperature,  $C$  for nanoparticle volume fraction,  $q_r$  for radiative heat flux.

Radiation heat flux  $q_r$  via Rosseland approximation can be set in the form (see Zaib et al [17]):

$$q_r = -\frac{4\sigma^*}{3k^*} \frac{\partial T^4}{\partial y} = -\frac{16\sigma^*}{3k^*} T^3 \frac{\partial T}{\partial y}, \tag{6}$$

where  $\sigma^*$  for Stefan–Boltzmann constant and  $k^*$  for coefficient of mean absorption.

The law of energy with radiation heat flux takes the form

$$u \frac{\partial T}{\partial x} + v \frac{\partial T}{\partial y} = \frac{\partial}{\partial y} \left[ \left( \alpha_1 + \frac{16\sigma^* T^3}{3k^*} \right) \frac{\partial T}{\partial y} \right] + \tau \left[ D_B \frac{\partial c}{\partial y} \frac{\partial T}{\partial y} + \frac{D_T}{T_\infty} \left( \frac{\partial T}{\partial y} \right)^2 \right]. \quad (7)$$

For the mathematical analysis of problem, we use the following transformation (see Ramesh [6])

$$u = bxf'(\eta), v = -\sqrt{bv} f(\eta), \eta = \sqrt{\frac{b}{v}} y, \\ T = T_\infty(1 + (\theta_w - 1)\theta(\eta)), \quad \phi(\eta) = \frac{c - c_\infty}{c_w - c_\infty}, \quad (8)$$

where  $\theta_w = \frac{T_w}{T_\infty}$ ,  $\theta_w > 1$  being the temperature ratio parameter.

After utilizing equation (8), equation (1) is identically satisfied and equations (2), (4) and (7) take the following form

$$\alpha f'''(\eta) - [f'(\eta)]^2 + f''(\eta)f(\eta) + \beta f''^2(\eta)f'''(\eta) - Mf'(\eta) = 0, \quad (9)$$

$$\left( \left( 1 + \frac{4}{3} Ra(1 + (\theta_w - 1)\theta(\eta))^3 \right) \theta'(\eta) \right)' + Pr \left( f(\eta)\theta'(\eta) + Nb\theta'(\eta)\phi'(\eta) + Nt\theta'^2(\eta) \right), \quad (10)$$

$$f''(\eta) + Le f(\eta)\phi'(\eta) + \frac{Nt}{Nb}\theta''(\eta) - \gamma\phi'(\eta) = 0, \quad (11)$$

with the boundary conditions

$$f(\eta) = 0, f'(\eta) = 1, \theta(\eta) = 1 + B\theta'(\eta), \phi(\eta) = 1 + D\phi'(\eta) \text{ at } \eta = 0, \\ f'(\eta) = 0, \theta(\eta) \rightarrow 0, \phi(\eta) \rightarrow 0 \text{ as } \eta = \infty, \quad (12)$$

where  $M = \frac{\sigma B_0^2}{\rho b}$  for magnetic parameter,  $\alpha = \frac{1}{\mu Ac}$  for Prandtl parameter,  $\beta = \frac{bU_w}{2c^2v}$  for elastic parameter,  $Pr = \frac{v}{\alpha_1}$  for Prandtl number,  $Ra = \frac{4\sigma^* T_\infty^3}{kk^*}$  for radiation parameter,  $Le = \frac{v}{D_B}$  for Lewis number,  $Nb = \frac{\tau D_B (C_w - C_\infty)}{v}$  for Brownian motion parameter,  $Nt = \frac{\tau D_T (T_w - T_\infty)}{T_\infty v}$  for thermophoresis parameter,  $\gamma = \frac{KU_w (C - C_\infty)}{v}$  for chemical reaction parameter,  $B = K_1 \sqrt{\frac{b}{v}}$  for

thermal slip parameter and  $D = K_2 \sqrt{\frac{b}{v}}$  for solutal slip parameter.

The physical quantities of interest like skin friction coefficient ( $C_{fx}$ ) local Nusselt number ( $Nu_x$ ) and local Sherwood number ( $Sh_x$ ) are defined as:

$$C_{fx} = \frac{\tau_w}{\rho U_w^2}, Nu_x = \frac{u_w q_w}{ka(T_w - T_\infty)} \text{ and } \\ Sh_x = \frac{u_w q_m}{aD_b(C_w - C_\infty)}, \quad (13)$$

where  $\tau_w$  is known as shear stress along the wall,  $q_w$  is known as heat flux,  $q_m$  is nanoparticle mass flux,

$$\tau_w = \frac{A}{c} \frac{\partial u}{\partial y} + \frac{A}{2c^3} \left( \frac{\partial u}{\partial y} \right)^3, \quad q_w = -k \frac{\partial T}{\partial y} \Big|_{y=0} \\ \text{and } q_m = -D \frac{\partial c}{\partial y} \Big|_{y=0}. \quad (14)$$

Dimensionless form of local skin friction coefficient ( $C_{fx}$ ), local Nusselt number ( $Nu_x$ ) and local Sherwood number ( $Sh_x$ ) are

$$\sqrt{Re} C_{fx} = [\alpha f''(\eta) + \beta f''(\eta)^3]_{\eta=0}, \quad \frac{Nu_x}{Re^{\frac{1}{2}}} = \\ - \left[ 1 + \frac{4}{3} Ra \theta_w^3 \right] \theta'(0), \quad \frac{Sh_x}{Re^{\frac{1}{2}}} = -\phi'(0), \quad (15)$$

where the local Reynolds number  $Re_x = \frac{U_w(x)}{av}$ .

### 3. Numerical solutions

Numerical scheme of non-linear differential equations (9)-(11) with conditions (12) corresponds to two-point boundary value problem. The solutions in closed form cannot be constructed due to highly non-linearity and coupled nature of govern system. Therefore, we developed the numerical results. We adopted the most effective fourth-fifth order Runge-Kutta-Fehlberg method through shooting procedure. The selection of suitable finite range of  $\eta_\infty$  is the most valuable part of this scheme. Tables 1 and 2 are constructed for comparative study of present results with those of previous results for various values of  $c$  and show a good agreement with each other.

### 4. Results and discussion

This section deals with the impact of various physical constraints on velocity  $f'(\eta)$ , temperature  $\theta(\eta)$  and concentration  $\phi(\eta)$ . Figure 1 is illustrating the variation of Prandtl parameter ( $\alpha$ ) on  $f'(\eta)$ ,  $\theta(\eta)$  and  $\phi(\eta)$ . As the value of Prandtl fluid parameter raised, the velocity of liquid and corresponding boundary layer increases. This is because by increasing Prandtl fluid parameter viscosity of fluid decreases. Consequently, fluid becomes less viscous for higher values of Prandtl fluid and velocity profiles increases. Further, we revealed both  $\theta(\eta)$  and  $\phi(\eta)$  and their associated thickness of boundary layers decrease with an increment Prandtl parameter.

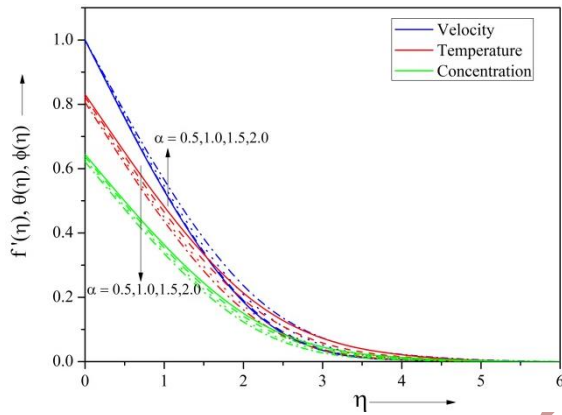


Fig. 1. Impact of  $\alpha$  on  $f'(\eta)$ ,  $\theta(\eta)$  and  $\phi(\eta)$ .

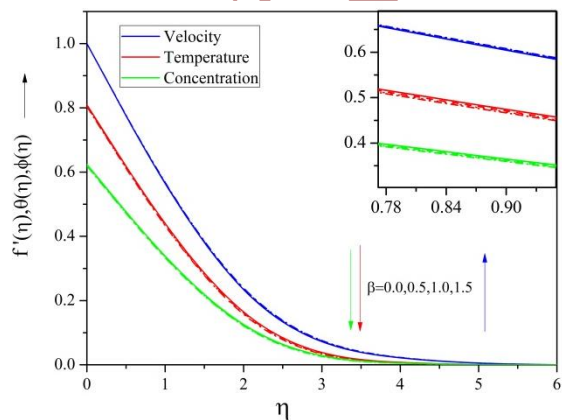


Fig. 2. Impact of  $\beta$  on  $f'(\eta)$ ,  $\theta(\eta)$  and  $\phi(\eta)$ .

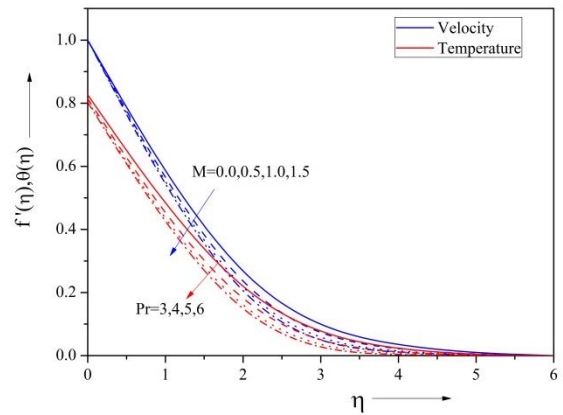


Fig. 3. Impact of  $M$  on  $f'(\eta)$  and  $Pr$  on  $\theta(\eta)$ .

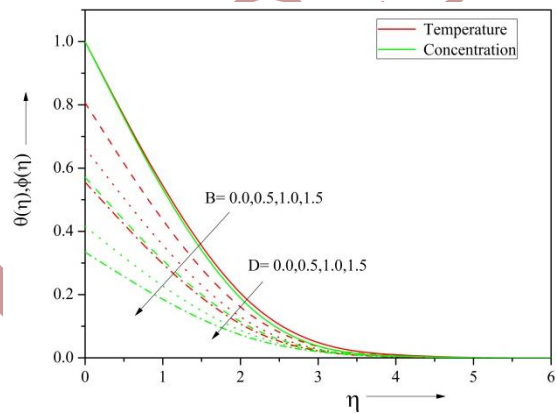


Fig. 4. Impact of  $B$  on  $\theta(\eta)$  and  $D$  on  $\phi(\eta)$ .

Variations of elastic parameter ( $\beta$ ) on  $f'(\eta)$ ,  $\theta(\eta)$  and  $\phi(\eta)$  are depicted in figure 2. It is revealed that a reduction is occurred in the  $f'(\eta)$  when the values of elastic parameter enhance. This type of behavior is validated because by increasing  $\beta$  viscosity increases which as an outcome gears down the velocity. But opposite behavior can be seen in temperature and concentration profile.

Figure 3 showing the importance of magnetic parameter ( $M$ ) on  $f'(\eta)$  and Prandtl number ( $Pr$ ) on  $\theta(\eta)$ . It is concluded that higher values of  $M$  lead to lower velocity. The reason is potentiality of Lorentz force which takes place due to magnetic field. This force restricts the flow intensity. Also in figure 3 we demonstrate the effect of ( $Pr$ ) on  $\theta(\eta)$ . It is noted that larger Prandtl number reduced the temperature.

Figure 4 illustrates the effect of thermal slip parameter ( $B$ ) on  $\theta(\eta)$ . We can observe that

the increasing value of thermal slip parameter reduces the thickness of thermal boundary layer and hence decrease the temperature. The coefficient of thermal accommodation is enhanced due to larger thermal slip parameter due to which a decrement is noticed in thermal efficiency towards the flow. Further figure 4 is also sketched to reveal the effects of solutal slip parameter ( $D$ ) on  $\phi(\eta)$ . This plot clearly demonstrates that  $\phi(\eta)$  decreases with increasing solutal slip parameter.

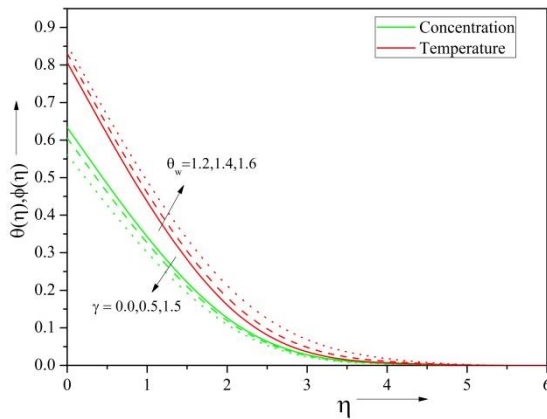


Fig. 5. Impact of  $\theta_w$  on  $\theta(\eta)$  and  $\gamma$  on  $\phi(\eta)$ .

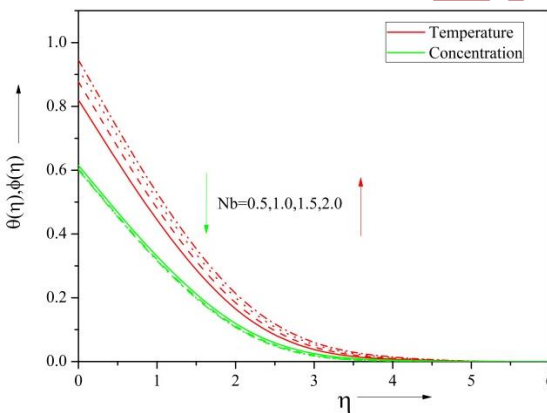


Fig. 6. Impact of  $Nb$  on  $\theta(\eta)$  and  $\phi(\eta)$ .

Figure 5 delineates the variations of  $\theta(\eta)$  versus  $\eta$  for various values of temperature ratio parameter ( $\theta_w$ ). We have visualized that an increase in  $\theta_w$  enhance  $\theta(\eta)$  and its associated layer thickness. Behavior of chemically reactive parameter ( $\gamma$ ) on  $\phi(\eta)$  is observed in figure 5. We visualized that  $\phi(\eta)$  and thickness of associated layer are decreasing while increase of  $\gamma$ . For the features of nanoparticle volume

mechanism, the nanoparticle volume field higher distortion is caused at  $\gamma = 1.0$ .

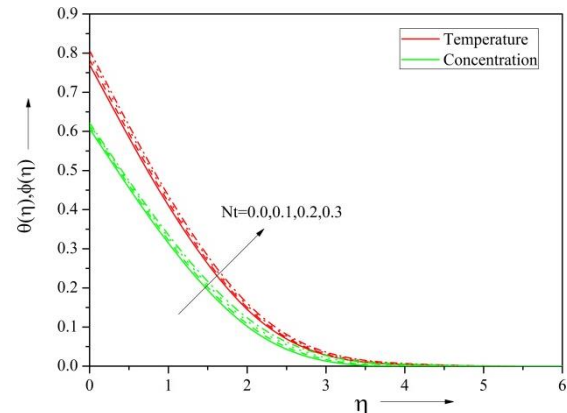


Fig. 7. Impact of  $Nt$  on  $\theta(\eta)$  and  $\phi(\eta)$ .

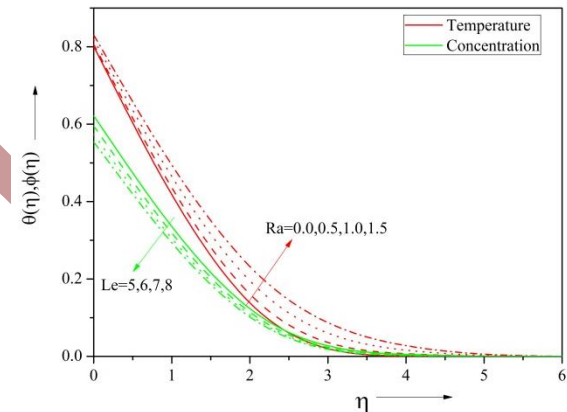


Fig. 8. Impact of  $Ra$  on  $\theta(\eta)$  and  $Le$  on  $\phi(\eta)$ .

Figure 6 portrays the effect of Brownian movement parameter ( $Nb$ ) on  $\theta(\eta)$  and  $\phi(\eta)$ . The temperature curves are higher for larger Brownian movement. As  $Nb$  increases, random motion of liquid particles increased that corresponds to more heat production. Thus temperature profiles show increasing behavior whereas the concentration profiles show opposite behavior. The impacts of thermophoresis parameter ( $Nt$ ) on  $\theta(\eta)$  and  $\phi(\eta)$  are depicted in Figure 7. From this plot, it can be examined that larger thermophoretic parameter is to increase  $\theta(\eta)$  and  $\phi(\eta)$ .

Figure 8 explains the characteristic of radiative parameter ( $Ra$ ) on  $\theta(\eta)$ . The higher radiative parameter gives an enhancement to temperature. More heat is generated in liquid due to radiation phenomenon that results in larger temperature. Further, figure 8 elucidates

**Table 1:** Comparison table of skin friction coefficient( $\alpha = \beta = 0$ ).

$M$	Akbar et al [13] (RKF method)	Cortell [10] (RK algorithm)	Present results (RKF-45 method)	Errors
1	-1.41421	-1.414	-1.41421	0.00000
5	-2.44948	-2.449	-2.44949	0.00001
10	-3.31662	-3.316	-3.31662	0.00000
50	-7.14142	-7.141	-7.14143	0.00001
500	-22.3830	-22.383	-22.38302	0.00002
1000	-31.6386	-31.638	-31.63858	0.00002

**Table 2:** Comparison of the result for Nusselt number  $-\theta'(0)$ .

$Pr$	Khan and Pop [3]	Wang [30]	Gorla and Sidawi [31]	Present result (RKF-45 method)	Errors
0.7	0.4539	0.4539	0.5349	0.45357	-0.00033
2	0.9113	0.9114	0.9114	0.91135	0.00005
7	1.8954	1.8954	1.8905	1.89539	-0.00001
20	3.3539	3.3539	3.3539	3.35387	-0.00003
70	6.4621	6.4622	6.4622	6.46209	-0.00001

**Table3:** Variation of skin friction coefficient, Nusselt number and Sherwood number for different physical parameter.

$B$	$D$	$\theta_w$	$\gamma$	$Le$	$M$	$Nb$	$Nt$	$Pr$	$Ra$	$\alpha$	$\beta$	$\sqrt{Re_x}C_f$	$-\frac{Sh_x}{\sqrt{Re_x}}$	$-\frac{Nu_x}{\sqrt{Re_x}}$
0	0.4	1.2	0.2	0.5	0.5	0.4	0.3	5	0.5	1	0.6	0.425488	0.947083	0.190698
0.5												0.409816	0.946238	0.124681
1												0.39773	0.946853	0.082593
0.3	0	1.2	0.2	0.5	0.5	0.4	0.3	5	0.5	1	0.6	0.419743	1.604065	0.081839
	0.5											0.415039	0.858037	0.15961
	1											0.413154	0.584691	0.202559
0.3	0.4	1.2	0.2	0.5	0.5	0.4	0.3	5	0.5	1	0.6	0.41563	0.946352	0.147669
		1.4										0.422245	0.956955	0.124959
		1.6										0.428982	0.965989	0.102936
0.3	0.4	1.2	0	0.5	0.5	0.4	0.3	5	0.5	1	0.6	0.415775	0.915744	0.146925
			0.5									0.415432	0.987935	0.148739
			1									0.415145	1.047913	0.150419
0.3	0.4	1.2	0.2	5	0.5	0.4	0.3	5	0.5	1	0.6	0.41563	0.946352	0.147669
				6								0.415392	1.011447	0.146891
				7								0.415156	1.06673	0.146968
0.3	0.4	1.2	0.2	0.5	0	0.4	0.3	5	0.5	1	0.6	0.49145	0.964897	0.166639
					0.5							0.41563	0.946352	0.147669
					1							0.284219	0.931216	0.133163
0.3	0.4	1.2	0.2	0.5	0.5	0.5	0.3	5	0.5	1	0.6	0.417295	0.962536	0.117544
						1						0.424469	0.990976	0.036334

						1.5						0.42999	0.997023	0.01069
0.3	0.4	1.2	0.2	0.5	0.5	0.4	0	5	0.5	1	0.6	0.408612	0.983517	0.264953
							0.1					0.411021	0.965947	0.217232
							0.2					0.413361	0.953892	0.178757
0.3	0.4	1.2	0.2	0.5	0.5	0.4	0.3	3	0.5	1	0.6	0.425187	0.948021	0.104965
								4				0.419522	0.945832	0.13088
								5				0.41563	0.946352	0.147669
0.3	0.4	1.2	0.2	0.5	0.5	0.4	0.3	5	0	1	0.6	0.408766	0.957383	0.074559
									0.5			0.41563	0.946352	0.147669
									1			0.421678	0.946355	0.185743
0.3	0.4	1.2	0.2	0.5	0.5	0.4	0.3	5	0.5	0.5	0.6	-0.34501	0.921984	0.124896
										1		0.41563	0.946352	0.147669
										1.5		0.907859	0.961428	0.162777
0.3	0.4	1.2	0.2	0.5	0.5	0.4	0.3	5	0.5	1	0	1.099521	0.939479	0.140804
											0.5	0.502964	0.945404	0.146706
											1	0.121264	0.949664	0.15107

**Table 4:** Values of Nusselt number for different values of the physical parameters when linear and nonlinear radiation.

$B$	$D$	$\gamma$	$Le$	$M$	$Nb$	$Nt$	$Pr$	$Ra$	$\alpha$	$\beta$	Linear $\frac{Nu_x}{\sqrt{Re_x}}$	Nonlinear $\frac{Nu_x}{\sqrt{Re_x}}$
0	0.4	0.2	0.5	0.5	0.4	0.3	5	0.5	1	0.6	0.138803	0.190698
0.5											0.081143	0.124681
1											0.049296	0.082593
0.3	0	0.2	0.5	0.5	0.4	0.3	5	0.5	1	0.6	0.043111	0.081839
	0.5										0.111325	0.15961
	1										0.152135	0.202559
0.3	0.4	0	0.5	0.5	0.4	0.3	5	0.5	1	0.6	0.099968	0.147669
		0.5									0.100638	0.124959
		1									0.101362	0.102936
0.3	0.4	0.5	5	0.5	0.4	0.3	5	0.5	1	0.6	0.100228	0.146925
			6								0.098082	0.148739
			7								0.096989	0.150419
0.3	0.4	0.5	0.5	0	0.4	0.3	5	0.5	1	0.6	0.11126	0.147669
				0.5							0.100228	0.146891
				1							0.091731	0.146968
0.3	0.4	0.2	0.5	0.5	0.5	0.3	5	0.5	1	0.6	0.072937	0.166639
					1						0.012659	0.147669
					1.5						0.001745	0.133163
0.3	0.4	0.2	0.5	0.5	0.4	0	5	0.5	1	0.6	0.212693	0.117544
						0.1					0.165202	0.036334
						0.2					0.128514	0.01069
0.3	0.4	0.2	0.5	0.5	0.4	0.3	3	0.5	1	0.6	0.086392	0.264953
							4				0.097146	0.217232
							5				0.100228	0.178757
0.3	0.4	0.2	0.5	0.5	0.4	0.3	5	0	1	0.6	0.084669	0.104965



								0.5			0.100228	0.13088
								1			0.093664	0.147669
0.3	0.4	0.2	0.5	0.5	0.4	0.3	5	0.5	0.5	0.6	0.086621	0.074559
									1		0.100228	0.147669
									1.5		0.109125	0.185743
0.3	0.4	0.2	0.5	0.5	0.4	0.3	5	0.5	1	0	0.095756	0.124896
										0.5	0.09961	0.147669
										1	0.102389	0.162777

that  $\phi(\eta)$  decreases as Lewis number increases. The physical argument behind this is the increase in Lewis number implies decrease in solute diffusivity which consequently reduces concentration profile and mass transfer rate.

Variations of skin friction coefficient, Nusselt and Sherwood numbers for various values of flow controlling parameters are reported numerically in Table 3. This table is evident to show the skin friction coefficient increases by increasing temperature ratio, Brownian movement, thermophoretic, radiation, elastic and Prandtl parameters. The higher values of thermal slip, solutal slip, chemical reaction, Lewis number and magnetic parameter caused a decrement in skin friction coefficient. Nusselt number is directly proportional to the temperature slip parameter, concentration slip parameter and Prandtl number, and is inversely proportional to magnetic, radiation, Brownian movement and thermophoretic parameters. Similarly, Sherwood number is directly proportional to concentration slip, Brownian movement and Prandtl number and it show opposite behavior for magnetic, radiation, Brownian movement and thermophoretic parameters. Table 4 represents numerical values of Nusselt number for the different values of the flow pertinent parameters in the presence linear and nonlinear thermal radiation parameter. Influence of all parameters on Nusselt number is similar to our observations as in Table 3. Further, it is interesting to note that, for all parameters, rate of heat transfer more in the presence nonlinear thermal radiation when compare to linear thermal radiation.

### 5. Conclusions

The main results of this study provided information regarding the velocity, temperature and concentration distribution of Prandtl

nanofluid. Finally, based on the present study we have some following important observations;

- Velocity temperature and concentration distributions and its layer thickness have same behavior for elastic parameter and Prandtl parameter.
- The increment in magnetic parameter corresponds to lesser thickness of momentum layer.
- The enhancement in temperature ratio and radiative parameters leads to larger temperature.
- Thermal and concentration slip parameters decrease the thicknesses of temperature and concentration boundary layers.
- Larger values of  $Nb$  and  $Nt$  temperature of fluid increases.
- Nonlinear thermal radiation is more effective when compare to liner thermal radiation.

**Acknowledgments:** The authors are very much thankful to the editor and referee for their encouraging comments and constructive suggestions to improve the presentation of this manuscript.

### References

- [1] S. U. S. Choi and J. A. Eastman, "Enhancing thermal conductivity of fluids with nanoparticles", *Proceedings of the ASME Int. Mech. Eng. Congress and Exposition*, Vol. 66, pp. 99–105, (1995).
- [2] J. Buongiorno, "Convective transport in nanofluids", *ASME J. Heat. Trans.*, Vol. 128, No. 3, pp. 240–250, (2005).
- [3] W. A. Khan and I. Pop, "Boundary-layer flow of a nanofluid past a stretching sheet", *Int.J. Heat and Mass Transfer*, Vol. 53, No. 11–12, pp. 2477–2483, (2010).

- [4] O. D. Makinde, W. A. Khan and Z. H. Khan, "Buoyancy effects on MHD stagnation point flow and heat transfer of a nanofluid past a convectively heated stretching/shrinking sheet", *Int. J. of Heat and Mass Transfer*, Vol. 6, No. 2, pp. 526–533, (2013).
- [5] M. Sheikholeslami, S. Abelman and D. D. Ganji, "Numerical simulation of MHD nanofluid flow and heat transfer considering viscous dissipation", *Int. J. Heat Mass Transfer*, Vol. 79, pp. 212–222, (2014).
- [6] G. K. Ramesh, "Numerical study of the influence of heat source on stagnation point flow towards a stretching surface of a Jeffrey nanofluid", *Journal of Engineering*. Vol. 2015, 10 pages, (2015).
- [7] G. K. Ramesh, S. A. Shehzad, T. Hayat and A. Alsaedi, "Activation energy and chemical reaction in Maxwell magneto-nanofluid with passive control of nanoparticle volume fraction", *Journal of the Brazilian Society of Mechanical Sciences and Engineering*, Vol. 40, pp. 422, (2018).
- [8] B. J. Gireesha, K. Ganesh Kumar, G. K. Ramesh, and B. C. Prasannakumara, "Nonlinear convective heat and mass transfer of Oldroyd-B nanofluid over a stretching sheet in the presence of uniform heat source/sink", *Results in Physics*, Vol. 9, pp. 1555–1563 (2018).
- [9] K. Goyardhan, G. Nagaraju, K. Kaladhar and M. Balasiddulu, "MHD and radiation effects on mixed convection unsteady flow of micropolar fluid over a stretching sheet", *Procedia Comp. Sci.*, Vol. 57, pp. 65–76, (2015).
- [10] R. Cortell, "A note on magnetohydrodynamic flow of a power-law fluid over a stretching sheet", *Appl. Math. Comput.* Vol. 168, pp. 557–566, (2005).
- [11] M. Y. Malik, T. Salahuddin, A. Hussain and S. Bilal, "MHD flow of tangent hyperbolic fluid over a stretching cylinder: Using Keller box method", *J. of Magnetism and Magnetic Materials*, Vol. 395, pp. 271–276, (2015).
- [12] R. Nasrin, S. Parvin and M. A. Alim, "Prandtl number effect on assisted convective heat transfer through a solar collector", *Applications and Applied Mathematics: An Int. J.*, Vol. 2, pp. 22–36, (2016).
- [13] N. S. Akbar, S. Nadeem, R. Ul Haq and Z. H. Khan, "Numerical solutions of Magneto hydrodynamic boundary layer flow of tangent hyperbolic fluid flow towards a stretching sheet with magnetic field", *Indian J. Phys.*, Vol. 87, No. 11, pp. 1121–1124, (2013).
- [14] R. Nasrin and M. A. Alim, "Prandtl number effect on free convective flow in a solar collector utilizing nanofluid", *Engg. Transac.*, Vol. 7, No. 2, pp. 62–72, (2012).
- [15] S. Nadeem, S. Ijaz and N. S. Akbar, "Nanoparticle analysis for blood flow of Prandtl fluid model with stenosis", *Int. Nano Letters*, Vol. 3, No. 35, pp. 2–13, (2013).
- [16] S. A. Shehzad, T. Hayat, A. Alsaedi and A. O. Mustafa, "Nonlinear thermal radiation in three-dimensional flow of Jeffrey nanofluid: A model for solar energy", *Appl. Math. And Compu.*, Vol. 248, pp. 273–286, (2014).
- [17] A. Zaib, M. M. Rashidi, A. J. Chamkha and N. F. Mohammad, "Impact of nonlinear thermal radiation on stagnation-point flow of a Carreau nanofluid past a nonlinear stretching sheet with binary chemical reaction and activation energy", *Proceedings of the Institution of Mechanical Engineers, Part C: Journal of Mechanical Engineering Science*. Vol. 232, No. 6, pp. 962–972, (2017).
- [18] T. Hayat, S. Qayyum, A. Alsaedi and S. A. Shehzad, "Nonlinear thermal radiation aspects in stagnation point flow of tangent hyperbolic nanofluid with double diffusive convection", *Journal of Molecular Liquids*, Vol. 223, pp. 969–978, (2016).

- [19]T. Hayat, T. Muhammad, A. Alsaedi and M.S. Alhuthali, "Magnetohydrodynamic three-dimensional flow of viscoelastic nanofluid in the presence of nonlinear thermal radiation", *J. Magnetism and Magnetic Materials*, Vol. 385, pp. 222–229, (2015).
- [20]G. K. Ramesh and B. J. Gireesha, "Flow over a stretching sheet in a dusty fluid with radiation effect", *ASME J. Heat transfer*, Vol. 135, No. 10, pp. 102702(1-6), (2013).
- [21]M. Mustafa, A. Mushtaq, T. Hayat, and A. Alsaedi, "Numerical study of the non-linear radiation heat transfer problem for the flow of a second-grade fluid", *J. Bulgarian Chemi. Commun.*, Vol. 47, No. 2, pp. 725-732, (2015).
- [22]G. K. Ramesh, A. J. Chamkha and B. J. Gireesha, "Boundary layer flow past an inclined stationary/moving flat plate with convective boundary condition", *Afrika Matematika*, Vol. 27. No. 1-2, pp. 87-95, (2016).
- [23]C. Y. Wang, "Flow due to a stretching boundary with partial slip an exact solution of the Navier-Stokes equations", *Chem. Eng. Sci.*, Vol. 57, pp. 3745–3747, (2002).
- [24]S. Mukhopadhyay and R. S. R. Gorla, "Effects of partial slip on boundary layer flow past a permeable exponential stretching sheet in presence of thermal radiation". *Heat Mass Trans.*, Vol. 45, pp. 1447–1452, (2009).
- [25]T. Fang, S. Yao, J. Zhang and A. Aziz, "Viscous flow over a shrinking sheet with a second order slip flow model". *Commun. Nonlinear Sci. and Numerical Simul.*, Vol. 15, No. 7, pp. 1831–1842, (2010).
- [26]K. Bhattacharyya, S. Mukhopadhyay and G. C Layek, "Slip effects on boundary layer stagnation-point flow and heat transfer towards a shrinking sheet", *Int. J. Heat and Mass Tran.*, Vol. 54, No. 1–3, pp. 308–313, (2011).
- [27]S. Das, R. N. Jana and O. D. Makinde, "MHD boundary layer slip flow and heat transfer of nanofluid past a vertical stretching sheet with non-uniform heat generation/absorption". *Int. J. Nanosci.*, Vol. 13, No. 3, 1450019 (2014).
- [28]M. Kezzar and M. Rafik Sari, "Series solution of nanofluid flow and heat transfer between stretchable/shrinkable inclined walls", *International Journal of Applied and Computational Mathematics*, Vol.3, No. 3, pp. 2231–2255, (2017).
- [29]M. Kezzar, M. Rafik Sari, R. Bourenane, M. M. Rashidi and A. Haihem, "Heat transfer in hydro-magnetic nano-fluid flow between non parallel plates using DTM", (2018). DOI: 10.22055/JACM.2018.24959.1221
- [30]C.Y. Wang, "Free convection on a vertical stretching surface", *J. Appl. Math. Mech. (ZAMM)*, Vol. 69, pp. 418–420, (1989).
- [31]R. S. R. Gorla and I. Sidawi, "Free convection on a vertical stretching surface with suction and blowing", *Appl. Sci. Res.*, Vol. 52, pp. 247–257, (1994).